Water Research 213 (2022) 118095

Contents lists available at ScienceDirect

Water Research

journal homepage: www.elsevier.com/locate/watres

Photochemical oxidation of phenols and anilines mediated by phenoxyl radicals in aqueous solution

Stephanie C. Remke [a,b], Tobias H. Bürgin [c], Lucie Ludvíková [d,e,f], Dominik Heger [d], Oliver S. Wenger [c], Urs von Gunten [a,b], Silvio Canonica [a,*]

[a] Eawag, Swiss Federal Institute of Aquatic Science and Technology, Überlandstrasse 133, Dübendorf, CH 8600, Switzerland
[b] School of Architecture, Civil and Environmental Engineering (ENAC), Ecole Polytechnique Fédérale de Lausanne (EPFL), Lausanne, CH 1015, Switzerland
[c] Department of Chemistry, University of Basel, Basel 4056, Switzerland
[d] Department of Chemistry, Faculty of Science, Masaryk University, Kamenice 5, Brno 62500, Czech Republic
[e] RECETOX, Faculty of Science, Masaryk University, Kamenice 5, Brno 62500, Czech Republic
[f] Present address: PASTEUR, Département de chimie, École normale supérieure, PSL University, Sorbonne University, CNRS, Paris 75005, France

ARTICLE INFO

Keywords:
Aquatic photochemistry
Phototransformation
Organic contaminant
Dissolved organic matter
Long-lived photooxidants

ABSTRACT

Reactive intermediates formed upon irradiation of chromophoric dissolved organic matter (CDOM) contribute to the degradation of various organic contaminants in surface waters. Besides well-studied "short-lived" photooxidants, such as triplet state CDOM (^{3}CDOM*) or singlet oxygen, CDOM-derived "long-lived" photooxidants (LLPO) have been suggested as key players in the transformation of electron-rich contaminants. LLPO were hypothesized to mainly consist of phenoxyl radicals derived from phenolic moieties in the CDOM. To test this hypothesis and to better characterize LLPO, the transformation kinetics of selected target compounds (phenols and anilines) induced by a suite of electron-poor model phenoxyl radicals was studied in aerated aqueous solution at pH 8. The phenoxyl radicals were generated by photosensitized oxidation of the parent phenols using aromatic ketones as photosensitizers. Under steady-state irradiation, the presence of any of the electron-poor phenols lead to an enhanced abatement of the phenolic target compounds (at an initial concentration of 1.0×10^{-7} M) compared to solutions containing the photosensitizer but no electron-poor phenol. A trend of increasing reactivity with increasing one-electron reduction potential of the electron-poor phenoxyl radical (range: 0.85–1.12 V vs. standard hydrogen electrode) was observed. Using the excited triplet state of 2-acetonaphthone as a selective oxidant for phenols, it was observed that the reactivity correlated with the concentration of electron-poor phenoxide present in solution. The rates of transformation of anilines induced by the 4-cyanophenoxyl radical were an order of magnitude smaller than for the phenolic target compounds. This was interpreted as a reduction of the radical intermediates back to the parent compound by the superoxide radical anion. Laser flash photolysis measurements confirmed the formation of the 4-cyanophenoxyl radical in solutions containing 2-acetonaphthone and 4-cyanophenol, and yielded values of $(2.6 - 5.3) \times 10^8$ M^{-1} s^{-1} for the second-order rate constant for the reaction of this radical with 2,4,6-trimethylphenol. These and further results indicate that electron-poor model phenoxyl radicals generated through photosensitized oxidation are useful models to understand the photoreactivity of LLPO as part of the CDOM.

1. Introduction

Dissolved organic matter (DOM)[1], a complex mixture of organic compounds ubiquitous in surface waters (Leenheer and Croué 2003; Zark and Dittmar 2018), is a key player in the sunlight-induced transformation of trace organic contaminants in the aquatic environment. Under sunlight, the chromophoric fraction of DOM, CDOM, generates photochemically produced reactive intermediates (PPRI), which can initiate the transformation of contaminants and thus contribute to their degradation (Richard and Canonica 2005; Vione et al. 2014). Besides well-studied short-lived PPRI, such as the excited triplet states of CDOM (^{3}CDOM*) (McNeill and Canonica 2016) or singlet oxygen ($^1O_2$) (Ossola

* Corresponding author.
E-mail address: silvio.canonica@eawag.ch (S. Canonica).
[1] For a list of abbreviations, see the Supplementary Information document

https://doi.org/10.1016/j.watres.2022.118095
Received 6 December 2021; Received in revised form 14 January 2022; Accepted 15 January 2022
Available online 19 January 2022

et al. 2021), long-lived photooxidants (LLPO), having lifetimes in the order of 10^{-4} s, have been proposed to occur upon irradiation of CDOM and to be relevant for the phototransformation of electron-rich contaminants in surface waters (Canonica and Freiburghaus 2001; Canonica and Hoigné 1995; Remke et al. 2021). The hypothesis that LLPO occur concomitantly with ^{3}CDOM* was able to explain the enhancement in CDOM-photosensitized transformation of electron-rich phenols, anilines and phenylureas when reducing their initial concentration from 5 μM down to 0.1 μM. The reason for this concentration dependence is that the target compound (TC, e.g., an electron-rich phenol) at higher concentrations, significantly affects the lifetime of LLPO. This leads to a lower steady-state concentration of LLPO at the higher TC concentrations with consequently lower pseudo-first-order transformation rate constant of the TC. In a recent study (Remke et al. 2021) we demonstrated that the effect of LLPO was correlated to the phenolic content of DOM and successfully tested a model system, consisting of a model photosensitizer and a model electron-poor phenol, to mimic the LLPO effect (Remke et al. 2021). These results supported the hypothesis that LLPO comprise DOM-derived phenoxyl radicals, whose precursors are electron-poor phenolic moieties of the DOM.

An important open question about LLPO model systems is related to the suitability of well-defined phenoxyl radicals to represent LLPO. This translates in identifying phenoxyl radicals with a sufficiently high reactivity with the above-mentioned electron-rich compounds. To date, a single phenoxyl radical, namely the 4-cyanophenoxyl radical (4-CN-PhO$^\bullet$), has been investigated using 3,4-dimethoxyphenol (DMOP) as a well-studied LLPO probe compound (Remke et al. 2021). Photochemically produced 4-CN-PhO$^\bullet$ was also shown to induce the oxidation of antimony(III) and arsenic(III) species (Buschmann et al. 2005a, Buschmann et al. 2005b), while phenoxyl radical was found to be unreactive toward antimony(III). Second-order rate constants for the reaction of various compounds with phenoxyl radicals, which are important oxidation intermediates of phenolic compounds in chemical and biological systems, have been determined over decades with methods such as, e.g., laser flash photolysis or pulse radiolysis (Neta and Grodkowski 2005). However, for electron-rich compounds showing an LLPO effect (Remke et al. 2021), rate constants in circumneutral aqueous solution are not available. An exception is the water-soluble vitamin E analogue 6-hydroxy-2,5,7,8-tetramethylchroman-2-carboxylic acid (trolox), for which values up to 4.1×10^8 $M^{-1}s^{-1}$ were reported (Neta and Grodkowski 2005). It is plausible to assume that the reactivity of phenoxyl radicals with a substrate correlates with the one-electron reduction potential ($E^0_{red,1}$) of the phenoxyl radicals (Li and Hoffman 1999, Lind et al. 1990, Steenken and Neta 2003). For basic aqueous solutions of various phenols, the second-order rate constants for the reactions between phenoxyl radicals and phenoxide ions were shown to be $\leq \approx 2 \times 10^9$ $M^{-1}s^{-1}$. Furthermore, a Marcus relationship was obtained, when they were plotted against the Gibbs free energy of the corresponding one-electron transfer reaction (Canonica and Tratnyek 2003). Based on these previous observations, such rate constants for a given TC are expected to increase with $E^0_{red,1}$ of the phenoxyl radicals and level off when $E^0_{red,1}$ approaches the one-electron reduction potential of the TC$^{\bullet+}$/TC couple. With such a model in mind, the selectivity of phenoxyl radicals reacting with TCs is expected to decrease with increasing $E^0_{red,1}$.

In the present study, the transformation kinetics of electron-rich model phenols and anilines as TCs was investigated by steady-state irradiation of aerated aqueous solutions containing, in addition to the TC, a model photosensitizer and an electron-poor phenol as model phenoxyl radical precursor. Several electron-poor phenols were used to generate phenoxyl radicals with various reduction potentials, and the ability of these radicals to represent LLPO was assessed. In addition, laser flash photolysis was utilized to clarify the photosensitized formation and decay of the 4-cyanophenoxyl radical, 4-CN-PhO$^\bullet$, in the presence of selected TCs, and to determine the second-order rate constant for the quenching of 4-CN-PhO$^\bullet$ by TMP.

2. Materials and methods

2.1. Chemicals and solutions

The following organic chemicals were used in this study: (A) Photosensitizers (Sens): 2-acetonaphthone (2-AN) and 4-carboxybenzophenone (CBBP); (B) Electron-poor phenols: 4-cyanophenol (4-CN-PhOH), 2,6-dichlorophenol, 3,5-dichlorophenol, 4-hydroxyacetophenone and 4-hydroxybenzoic acid; (C) Target compounds: aniline, 3,4-dimethoxyphenol (DMOP), 4-methylaniline and 2,4,6-trimethylphenol (TMP); (D) Further compounds: acetonitrile, 4-nitroanisole and pyridine. Inorganic chemicals used as buffer components comprised boric acid, phosphoric acid, $Na_2HPO_4{\cdot}2H_2O$ and $NaH_2PO_4{\cdot}H_2O$. All chemicals were purchased from common commercial suppliers as detailed in the Supplementary Information (SI), Text S1 and used as received. Ultrapure water with a resistivity of > 18.2 MΩ·cm was obtained from an Arium® pro ultrapure water system (Sartorius AG, Göttingen Germany) except for laser flash photolysis experiments (for details see Text S1, SI). For all compounds, stock solutions of appropriate concentrations were prepared in ultrapure water except for 2-acetonaphthone, for which a 40/60 (v/v) acetonitrile/water mixture was utilized. The maximum concentration of acetonitrile in irradiated solutions was always lower than 2% (v/v) in nanosecond laser flash photolysis and lower than 0.2% (v/v) in steady-state irradiation experiments and assumed to have no significant effect on the studied reactions.

2.2. Photosensitized formation of electron-poor phenoxyl radicals

In a previous study (Remke et al. 2021) solutions containing a photosensitizer (2-AN) and an electron-poor phenol (4-cyanophenol) were employed as surrogates for CDOM solutions to produce, under irradiation, on the one hand excited triplet states of the photosensitizer (^{3}Sens*, as models for ^{3}CDOM*), and on the other hand an electron-poor phenoxyl radical (as model for LLPO). Such a model system and its analogy to CDOM is represented in Fig. 1.

The two employed aromatic ketone photosensitizers, 2-AN and CBBP (see (A) above), were chosen due to the suitability of their excited triplet states to model ^{3}CDOM* (Canonica et al. 1995; Carena et al. 2019). Moreover, the $E^0_{red,1}$ values of ^{3}Sens* for these two model photosensitizers (i.e., 1.34 and 1.84 V vs. standard hydrogen electrode (SHE), respectively) represent a lower and upper limit, respectively, for the estimated range of one-electron reduction potentials of ^{3}CDOM* (McNeill and Canonica 2016). The five electron-poor phenols (R-PhOH$_{ep}$) (see (B) above) were selected to confirm the enhancement effect on TC transformation previously observed using 4-cyanophenol and to test in particular the lower limit of the range of $E^0_{red,1}$ estimated for LLPO (i.e., ~1.0−1.3 V vs. SHE (Remke et al. 2021)). These phenols are represented in Fig. 2a, together with $E^0_{red,1}$(R-PhO$_{ep}^\bullet$/R-PhO$_{ep}^-$) of the corresponding phenoxyl radicals (R-PhO$_{ep}^\bullet$), covering the range of 0.85−1.12 V vs. SHE (see Text S4 and Table S2b (SI) for details). Also represented in Fig. 2a is the fraction of phenoxide (R-PhO$_{ep}^-$), $f_{R-PhO_{ep}^-}$, at pH 8.0, since this is an important parameter for the formation of R-PhO$_{ep}^\bullet$ from the reaction of ^{3}Sens* with the phenols, as illustrated in Fig. 2b. The formation of R-PhO$_{ep}^\bullet$ from undissociated phenols and phenoxides can be described by Eqs. (1), (2) and (3), respectively.

$$^3\text{Sens}^* + \text{R-PhOH}_{ep} \rightarrow \text{Sens}^{\bullet-} + \text{R-PhOH}_{ep}^{\bullet+} \quad (1)$$

$$\text{R-PhOH}_{ep}^{\bullet+} \rightarrow \text{R-PhO}_{ep}^\bullet + \text{H}^+ \quad (2)$$

$$^3\text{Sens}^* + \text{R-PhO}_{ep}^- \rightarrow \text{Sens}^{\bullet-} + \text{R-PhO}_{ep}^\bullet \quad (3)$$

The reaction of excited triplet aromatic ketones with phenols (Canonica et al., 2000) and phenoxides (Das and Bhattacharyya, 1981) has been shown to consist of a rate-determining single electron transfer (Eqs. (1) and ((3), respectively). Therefore, a diffusion-controlled

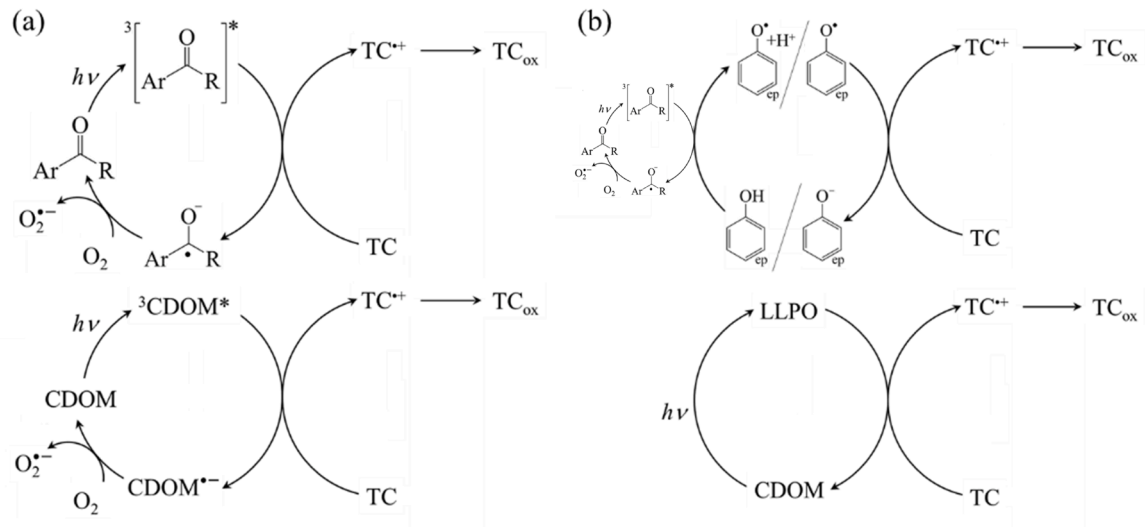

Fig. 1. Scheme of the main reactions involved in the phototransformation of a target compound (TC) in aerated aqueous solution through (a) excited triplet states of a model photosensitizer, represented by a ketone (upper part) or ^{3}CDOM* (lower part), and (b) an electron-poor phenoxyl radical (upper part) or LLPO (lower part). In (a), the re-cycling of the photosensitizer or CDOM involves molecular oxygen with an ensuing superoxide radical anion production.

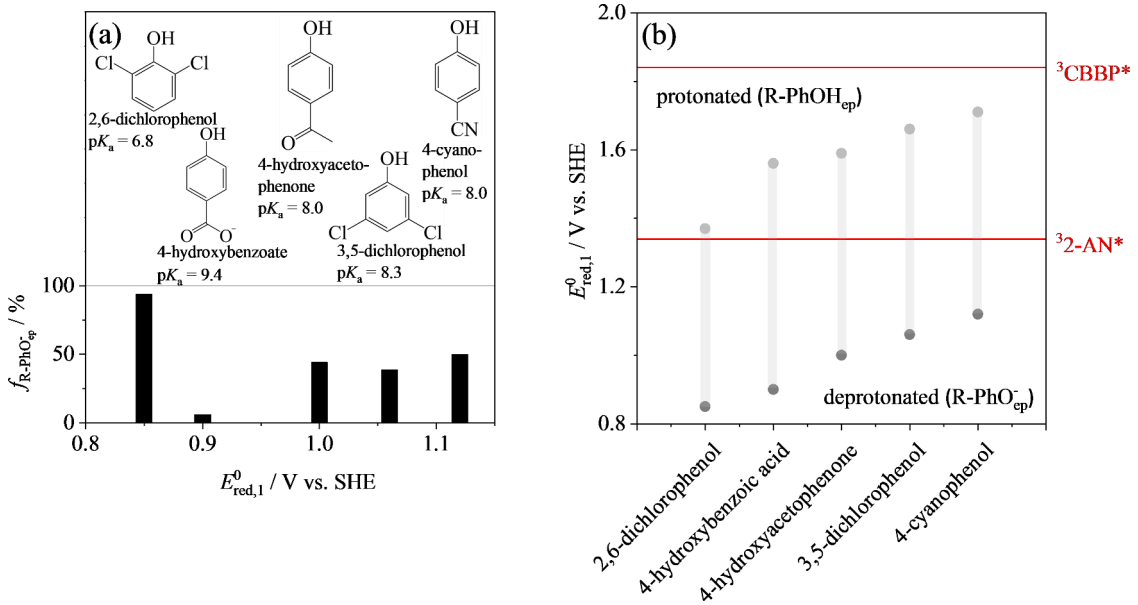

Fig. 2. (a) Structures, pK_a, one-electron reduction potential ($E^0_{red,1}$(R-PhO$_{ep}^{\bullet}$/R-PhO$_{ep}^-$), x-axis), and phenoxide fraction at pH 8.0 ($f_{R-PhO_{ep}^-}$, vertical bars) of the studied electron-poor phenols. (b) One-electron reduction potential of the couples R-PhOH$_{ep}^{\bullet+}$/R-PhOH$_{ep}$ (light grey circles) and R-PhO$_{ep}^{\bullet}$/R- PhO$_{ep}^-$ (dark grey circles) compared to those of the excited triplet state of CBBP and 2-AN (horizontal red lines).

reaction for the undissociated phenols is expected when $E^0_{red,1}$ (^{3}Sens*) > $E^0_{red,1}$ (R-PhOH$_{ep}^{\bullet+}$/R-PhOH$_{ep}$), and for the phenoxides when $E^0_{red,1}$ (^{3}Sens*) > $E^0_{red,1}$ (R-PhO$_{ep}^{\bullet}$/R-PhO$_{ep}^-$) (Canonica et al., 2000). Fig. 2b shows that the excited triplet state of CBBP, ^{3}CBBP*, fulfils this condition for all studied undissociated phenols and phenoxides, but the excited triplet state of 2-AN, ^{3}2-AN*, fulfils the condition only for phenoxides. Therefore, the production rate of electron-poor phenoxyl radicals from reaction with ^{3}2-AN* is expected to positively correlate with $f_{R-PhO_{ep}^-}$.

2.3. Steady-state irradiation experiments

Aqueous solutions (16 mL) containing 5.0 mM phosphate buffer (pH=8.0 ± 0.1) and appropriate concentrations of a photosensitizer, an electron-poor phenol, and a target compound were prepared in ultrapure water and transferred to quartz tubes (18 mm external diameter and 15 mm internal diameter). Prior to irradiation, the tubes were placed in a water bath for 15 min at 25 °C. Irradiation experiments were conducted as described in detail elsewhere (Remke et al., 2021). Briefly, the quartz tubes containing the experimental solutions were irradiated in a temperature-controlled (25.0 ± 0.2 °C) merry-go-round photoreactor equipped with a medium-pressure mercury lamp placed in a borosilicate cooling jacket at the center of the reactor. The tubes were immersed in a filter solution containing 0.15 M sodium nitrate, which, combined with the cooling jacket, absorbed all light of wavelength λ < 320 nm. During irradiations, which lasted overall between 3 and 36 min, seven aliquots (360 μL) of solution were withdrawn from the quartz tubes at equidistant time intervals during the irradiation. The photon fluence rate in the tubes was determined weekly using the 4-nitroanisole/pyridine chemical actinometer as described elsewhere (Leresche

et al. 2016). The photon fluence rate in the wavelength band of 334−436 nm varied in the range of (4.4−5.6) × 10^{-3} einstein m^{-2} s^{-1} over the duration of this study (calculations according to (Laszakovits et al. 2017; Leresche et al. 2016) Text S2, SI). Pseudo-first-order rate constants, k^{obs} (s^{-1}), for the transformation of a TC were obtained by linear regression as the slope of natural logarithmic concentration values of TC versus time. No light screening correction was applied due to the negligible absorbance of the investigated solutions at λ > 320 nm.

2.4. Analytical methods

Compound concentrations were determined by high-performance liquid chromatography (HPLC) using an Agilent 1100 HPLC system equipped with UV-vis absorbance and fluorescence detection. Typically, for samples taken from experiments with ≥ 1 μM initial target compound concentration the UV-vis absorbance detector was employed, while for samples with submicromolar initial concentrations the fluorescence detector was often applied, because higher sensitivity could be achieved for most compounds. Details on the HPLC set-up and methods are provided in Text S3 and Table S2a–c (SI).

The pH of the samples was measured before and after each irradiation experiment using a pH meter (a Metrohm Model 605 equipped with a Metrohm pH electrode Model 6.02341.110). A small pH decrease (< 0.1 pH units) was observed during most of the irradiation experiments.

2.5. Nanosecond laser flash photolysis

Laser flash photolysis experiments were performed utilizing two distinct instruments described below as LFP-1 and LFP-2.

(1) LFP-1: An Nd:YAG laser (Quantel Brilliant, pulse length ~10 ns, pulse energy ~ 10 mJ (energy measured at the cuvette), emission wavelength 355 nm) with a 2X beam expander from Thorlabs was employed to excite an area of 1 × 1 cm of the samples in a 1 × 1 × 4 cm quartz cuvette. Transient absorption spectra were recorded on an LP-920 KS setup from Edinburg Instruments, equipped with an ICCD camera from Andor (with time integration over 200 ns). A photomultiplier tube was used to record kinetic transient absorption traces at single wavelengths. Experiments were performed at 25 °C in a temperature-controlled cuvette holder.

(2) LFP-2: The setup of this equipment is described in detail elsewhere (Leresche et al., 2019). Briefly, an Nd:YAG laser (EKSPLA, model SL334, pulse length < 150 ps, pulse energy ~150 mJ (measured directly after the laser), emission wavelength 355 nm) was employed to excite the sample in a 4 × 1 × 1 cm quartz cuvette. The laser pulse was dispersed using a cylindrical concave lense on one 4 × 1 cm side of the cuvette. Transient absorption spectra were recorded using an ICCD camera (Andor iStar, model DH740i-18U-03) with an overpulsed Xenon arc lamp as source of the probe light. Kinetic transient absorption traces were recorded using the software TekScope on a Tektronix digital phosphor oscilloscope (model DPO7104C) employing a Hamamatsu model 928 photomultiplier tube. Experiments were performed in an air-conditioned room at an ambient temperature of 20 ± 1 °C.

The Software Origin 2019b (Academic) (OriginLab Corporation) was employed for the data analysis. Transient absorption spectral data were plotted and absorption bands were ascribed to transient species based on previous observations (Table S5, SI). Kinetic transient absorption traces were fitted to single exponential decays. Fitting of kinetic traces of ^{3}2-AN* at 450 or 440 nm was performed using absorbance data, typically up to 8–10 μs time delay after the laser pulse. To fit kinetic traces of 4-CN-PhO$^\bullet$ at 436 nm, the fitting range was set to 5−100 or 5−400 μs after the laser pulse, to avoid the early signal by ^{3}2-AN*. Fitting residuals were examined for every trace visually and concluded to be adequate (Figs. S12–17, SI).

The software Kintecus© (Ianni, 2017) was employed for kinetic simulations to verify the set of assumed reactions occurring after the laser pulse (Text S5, Fig. S9, Table S6, SI).

3. Results and discussion

3.1. Target compound transformation induced by electron-poor phenoxyl radicals

The photosensitized transformation of the phenolic TCs DMOP and TMP, measured at initial TC concentrations of 0.1 and 5.0 μM in the presence of either CBBP or 2-AN as photosensitizers and one of the five selected electron-poor phenols, followed first-order kinetics. The corresponding pseudo-first-order rate constants (k^{obs}; note that in this paper $k^{obs}_{0.1}$ and $k^{obs}_{5.0}$ are used to designate the rate constants for the initial TC concentrations of 0.1 and 5.0 μM, respectively) for the investigated different combinations of TC, photosensitizer, and electron-poor phenol are shown in Fig. 3 (for values, see Tables S4a and S4b, SI). The concentrations of the photosensitizers and electron-poor phenols were also monitored during these irradiation experiments and found to remain unchanged within the analytical uncertainty (± 5%) during the time span for the determination of $k^{obs}_{0.1}$. A limited decrease in the concentration of these components (< 15% over 30 min) was found for experiments used to determine $k^{obs}_{5.0}$, which can be considered as negligible

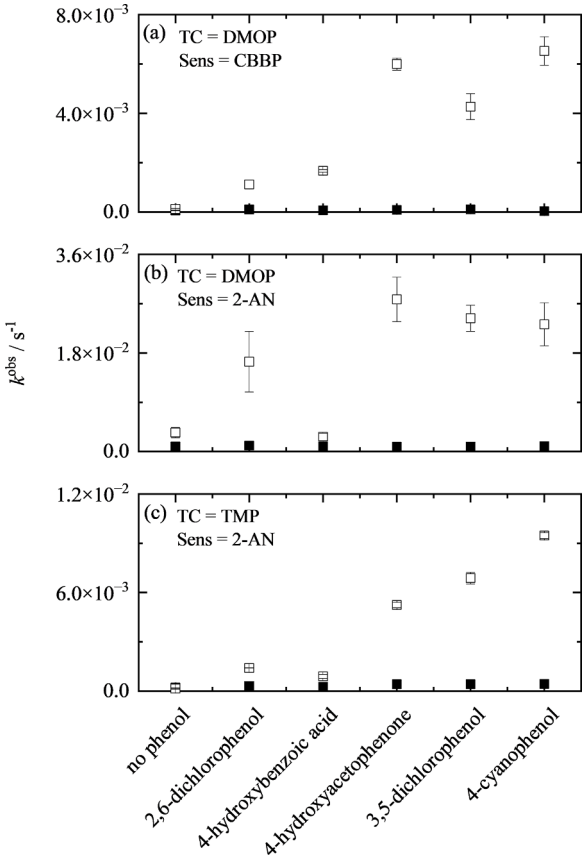

Fig. 3. Pseudo-first-order rate constants for the photosensitized transformation of (a and b) DMOP and (c) TMP determined at pH 8.0 and 25 °C for irradiated solutions containing (a) CBBP (0.5 μM) or (b and c) 2-AN (1.5 μM) and a suite of electron-poor phenols (5.0 μM) indicated on the x-axis of the diagrams. Values with no added electron-poor phenol are also provided (no phenol on x-axis). Open squares: Experimental data for an initial TC concentration of 0.1 μM; filled squares: Experimental data for an initial TC concentration of 5.0 μM. Symbols represent average values from duplicate experiments, while error bars indicate the corresponding mean deviations.

compared to the variation in photon fluence rate (Section 2.3). In general, much higher $k_{0.1}^{obs}$ values were obtained compared to $k_{5.0}^{obs}$. Using the kinetic considerations about LLPO mentioned in the Introduction and explained in detail in our previous studies (Canonica and Hoigné 1995; Canonica and Freiburghaus 2001; Remke et al. 2021), this enhancement is interpreted as being due to long-lived reactive species formed in the presence of electron-poor phenols. The involved species are presumably the corresponding electron-poor phenoxyl radicals. A previous kinetic analysis of the system DMOP/2-AN/4-cyanophenol revealed that, at 5.0 μM initial DMOP concentration, only 14% of the observed DMOP transformation was due to 4-CN-PhO$^{\bullet}$, while for an initial DMOP concentration of 0.1 μM this fraction increased to 89% (Remke et al. 2021), which supports the present interpretation. Moreover, $k_{5.0}^{obs}$ values for each TC/photosensitizer combination were low and not significantly affected by the presence of electron-poor phenol, confirming the assumption that, at an initial TC concentration of 5.0 μM, TC transformation is primarily due to ^{3}Sens*, while electron-poor phenoxyl radicals play a minor role.

For the investigated combinations of TCs and electron-poor phenols, a series of control irradiation experiments was performed using solutions that contained no photosensitizer. The $k_{0.1}^{obs}$ and $k_{5.0}^{obs}$ values obtained from these experiments, named $k_{0.1,control}^{obs}$ and $k_{5.0,control}^{obs}$, respectively, (see Table S4a, SI), were at least one order of magnitude smaller than for solutions containing 2-AN, except for the pair DMOP (0.1 μM)/4-hydroxybenzoic acid (only factor of ~4.6 smaller). Compared to solutions containing CBBP, k^{obs} values from control experiments were also clearly smaller, but the differences were less important for the pairs DMOP (0.1 μM)/4-hydroxybenzoic acid (factor of ~2.8 smaller) and DMOP (0.1 μM)/4-hydroxyacetophenone (factor of ~3.3 smaller). This suggests that, for these two electron-poor phenols, a secondary photochemical process, besides Eqs. (1)–(3), generates the corresponding phenoxyl radicals. We propose that this secondary source of phenoxyl radicals is caused by photoionization of the corresponding phenoxides (Eq. (4)), since their UV absorption spectra (Fig. S3, SI) overlap with the spectrum of UV light in the photoreactor.

$$R\text{-}PhO_{ep}^{-} + h\nu \rightarrow R\text{-}PhO_{ep}^{\bullet} + e_{aq}^{-} \quad (4)$$

To explore possible correlations of k^{obs} with molecular parameters of the electron-poor phenols, such as $E_{red,1}^0$(R-PhO$_{ep}^{\bullet}$/R-PhO$_{ep}^{-}$) or $f_{R-PhO_{ep}^{-}}$, it is convenient to consider exclusively the contribution to TC transformation due to electron-poor phenoxyl radicals produced according to Eqs. (1)–(3). This is done by subtracting the corresponding values obtained from control experiments, $k_{0.1,control}^{obs}$ from the original $k_{0.1}^{obs}$ values (which eliminates the contribution of Eq. (4) to k^{obs}). In addition, the k^{obs} values for an initial TC concentration of 5.0 μM for irradiated solution with photosensitizer but without electron-poor phenol ($k_{5.0,Sens}^{obs}$) should be subtracted (which eliminates the contribution of ^{3}Sens* to k^{obs}). No correction was made to compensate for direct photolysis of TC, since this was negligible (data in Table S4a, SI). The values for these corrected rate constants, $k_{R-PhO_{ep}^{\bullet}}^{obs,c}$ (= $k_{0.1}^{obs} - k_{0.1,control}^{obs} - k_{5.0,Sens}^{obs}$), are also displayed in Tables S4a and S4b (SI).

To carry out this data analysis, first, the data for the CBBP-photosensitized transformation of DMOP in the presence of various electron-poor phenols were considered (Fig. 3a). As shown in Fig. 4a, the corrected pseudo-first-order rate constants, $k_{R-PhO_{ep}^{\bullet}}^{obs,c}$ exhibited a significant positive and linear correlation to $E_{red,1}^0$(R-PhO$_{ep}^{\bullet}$/R-PhO$_{ep}^{-}$), with coefficient of determination $R^2 = 0.93$ (details of the linear regression are provided in Table S4f, SI). $k_{R-PhO_{ep}^{\bullet}}^{obs,c}$ increased by a factor of ~6 over a reduction potential span of ~0.3 V. For this data set, it can be assumed that ^{3}CBBP* reacts with all of the electron-poor phenols (independent of the speciation of the latter) at approximately the same rate, which should be close to a diffusion-controlled reaction (Section 2.2). For any of the electron-poor phenols, the phenoxyl radical yield may be safely assumed to be close to unity, as previously observed for a variety of substituted phenols (Das and Bhattacharyya 1981). This results in a phenoxyl radical production rate that is independent of the employed electron-poor phenol. Therefore, the increase in $k_{R-PhO_{ep}^{\bullet}}^{obs,c}$ as a function of the $E_{red,1}^0$(R-PhO$_{ep}^{\bullet}$/R-PhO$_{ep}^{-}$) is mainly attributed to the increased reactivity of the phenoxyl radicals with the TC (in this case DMOP), which qualitatively fulfils the expectation.

Since 2-AN should be capable of oxidizing all studied phenoxides but not their corresponding undissociated phenols (see Fig. 2b), $k_{R-PhO_{ep}^{\bullet}}^{obs,c}$ values for the 2-AN-photosensitized transformation of DMOP (derived from Fig. 3b) are expected to be affected by both $E_{red,1}^0$(R-PhO$_{ep}^{\bullet}$/R-PhO$_{ep}^{-}$) (as seen above with CBBP) and $f_{R-PhO_{ep}^{-}}$. To factor out the dependence of $k_{R-PhO_{ep}^{\bullet}}^{obs,c}$ on $E_{red,1}^0$(R-PhO$_{ep}^{\bullet}$/R-PhO$_{ep}^{-}$), we assumed it to

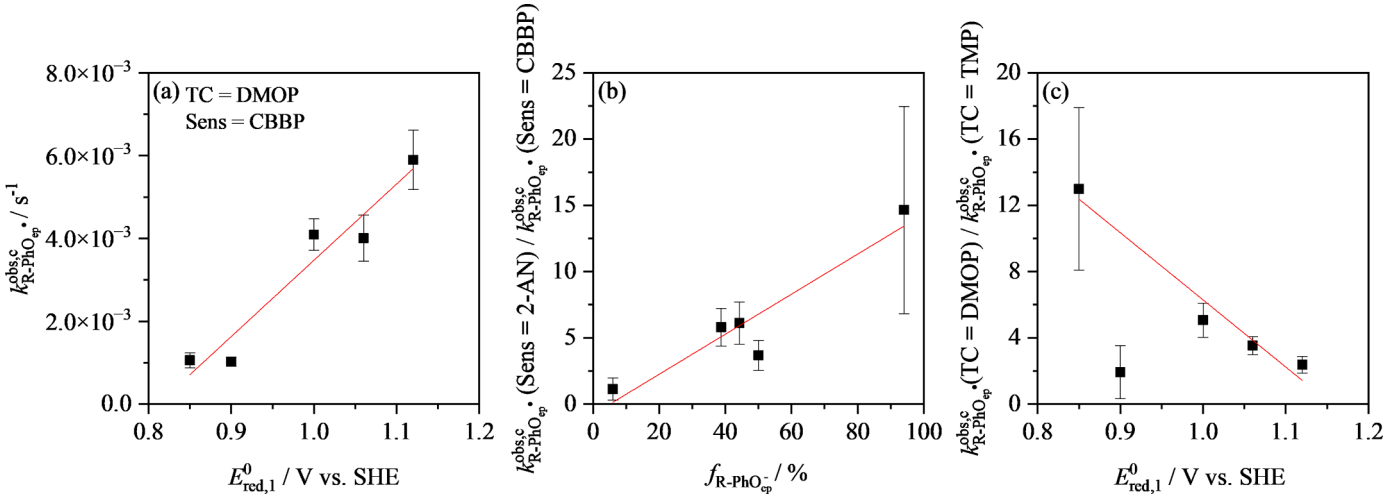

Fig. 4. (a) Corrected pseudo-first-order rate constants, $k_{R-PhO_{ep}^{\bullet}}^{obs,c}$, obtained for the transformation of 3,4-dimethoxyphenol (DMOP) photosensitized by 4-carboxybenzophenone (CBBP) in the presence of various electron-poor R-PhOH as a function of the one-electron reduction potential of the corresponding phenoxyl radical, $E_{red,1}^0$(R-PhO$_{ep}^{\bullet}$/R-PhO$_{ep}^{-}$). (b) Ratio of $k_{R-PhO_{ep}^{\bullet}}^{obs,c}$ for DMOP transformation with 2-AN and CBBP as photosensitizers, respectively, as a function of the fraction of deprotonated R-PhOH$_{ep}$, $f_{R-PhO_{ep}^{-}}$. (c) Ratio of $k_{R-PhO_{ep}^{\bullet}}^{obs,c}$ for the 2-AN-photosensitized transformation of DMOP and TMP, respectively, as a function of the $E_{red,1}^0$(R-PhO$_{ep}^{\bullet}$/R-PhO$_{ep}^{-}$).

be identical as in the above case with CBBP. Consequently, $k^{obs,c}_{R-PhO_{ep}\bullet}$ values obtained with 2-AN were divided by those obtained with CBBP. These $k^{obs,c}_{R-PhO_{ep}\bullet}$ ratios, i.e., $k^{obs,c}_{R-PhO_{ep}\bullet}$(Sens = 2-AN) / $k^{obs,c}_{R-PhO_{ep}\bullet}$(Sens = CBBP), are represented in Fig. 4b. They are linearly and positively correlated (R^2 = 0.88) to $f_{R-PhO_{ep}^-}$ (calculated according to the details provided in Text S4 and in Table S3c, SI). In the case of 4-CN-PhOH, these results concur with the observed pH dependence of the transformation kinetics of this phenol photosensitized by 2-AN (Wenk et al., 2021).

The set of $k^{obs,c}_{R-PhO_{ep}\bullet}$ data obtained for DMOP and TMP with 2-AN as a photosensitizer (Figs. 4c and 3a,b for uncorrected data) were compared to obtain information about the selectivity of the various R-$PhO_{ep}^{\bullet}$ in their reaction with these two phenolic TCs. The ratio of $k^{obs,c}_{R-PhO_{ep}\bullet}$ values obtained for DMOP and TMP, respectively, i.e., $k^{obs,c}_{R-PhO_{ep}\bullet}$(TC = DMOP)/ $k^{obs,c}_{R-PhO_{ep}\bullet}$(TC = TMP)(Fig. 4c) decreases linearly (R^2 = 0.96) with $E^0_{red,1}$(R-$PhO_{ep}^{\bullet}$/R-PhO_{ep}^-) from ~13 (at 0.85 V) to ~2 (at 1.12 V), indicating a marked loss in selectivity of R-$PhO_{ep}^{\bullet}$ with increasing $E^0_{red,1}$(R-$PhO_{ep}^{\bullet}$/R-PhO_{ep}^-). The higher reactivity of DMOP compared to TMP is due to the lower tendency of TMP to undergo oxidation, corresponding to a higher reduction potential of the couple $TMP^{\bullet+}$/TMP compared to $DMOP^{\bullet+}$/DMOP (see SI, Table 3a). Note that the value of the $k^{obs,c}_{R-PhO_{ep}\bullet}$ ratio for 4-hydroxybenzoic acid, the lowest point in Fig. 4c, is considered as an outlier, explainable by a high relative error due to the small measured rate constants. Since $k^{obs,c}_{R-PhO_{ep}\bullet}$ values for DMOP are always higher than for TMP (except for the mentioned outlier), one can also infer that for any studied R-$PhO_{ep}^{\bullet}$, the second-order rate constant for their reaction with TMP must be lower than the limiting value of a diffusion-controlled reaction.

3.2. *Transformation of 2,4,6-trimethylphenol and aniline induced by the 4-cyanophenoxyl radical*

The characterization of the LLPO model system using 2-AN as a photosensitizer and 4-cyanophenol as a phenoxyl radical precursor, accomplished for DMOP in a preceding study (Remke et al. 2021), was extended here to other TCs (TMP and aniline). First, irradiation experiments were performed at initial TC concentrations of 0.1 and 5.0 μM with various concentrations of 4-cyanophenol in the range of 0–10 μM. The corresponding k^{obs} are presented in Fig. 5a,b (see also Fig. S4, SI). During each kinetic run, the concentrations of 2-acetonaphthone and 4-cyanophenol remained almost constant (± 5% with 0.1 μM initial concentration and ± 15% with 5.0 μM initial concentration) (Fig. S5, SI).

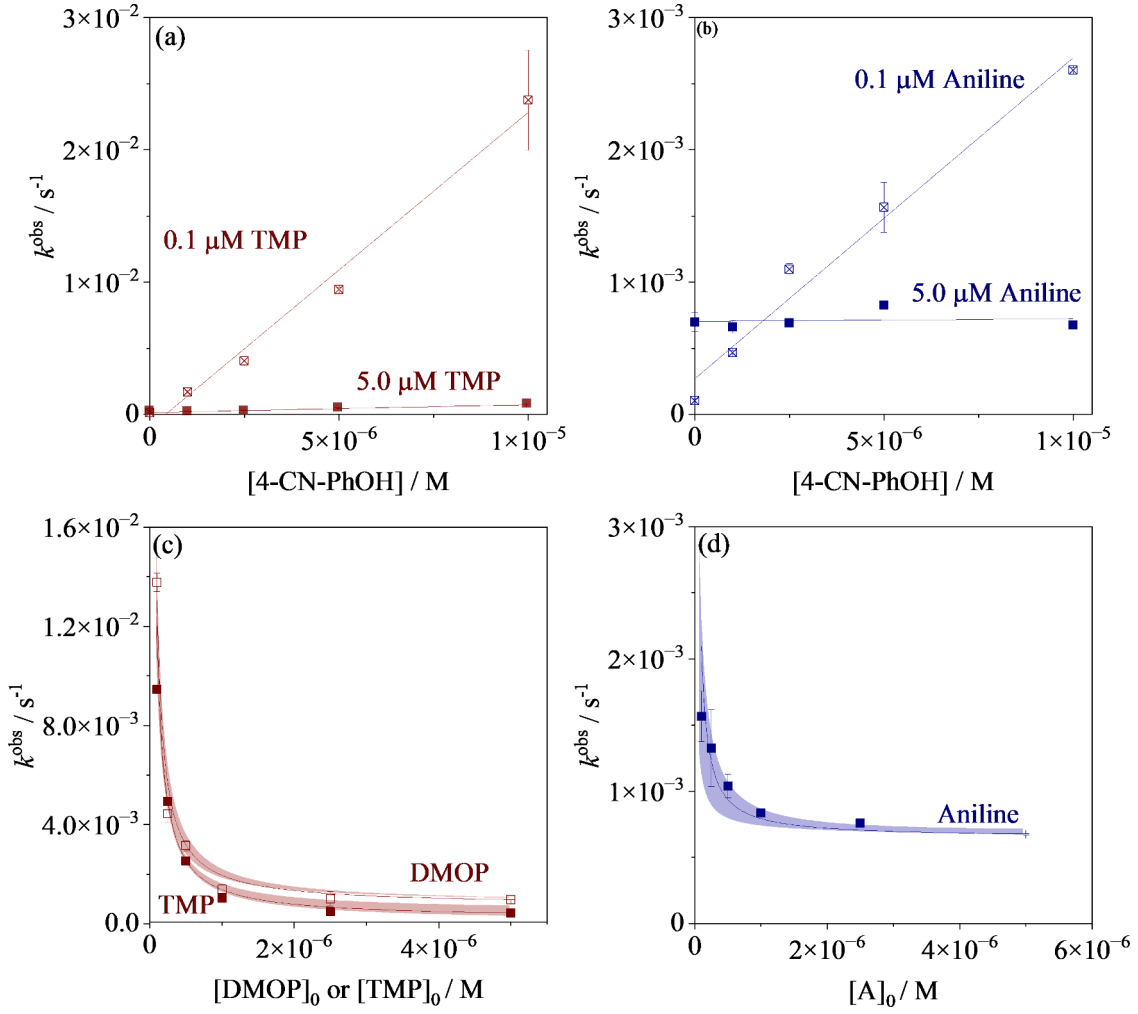

Fig. 5. Pseudo-first-order rate constants, k^{obs}, determined at pH 8.0 and 25.0 °C for the transformation of (a, c) 2,4,6-trimethylphenol (TMP) and (b,d) aniline (A) photosensitized by 2-acetonaphthone (1.5 μM). Experiments performed using (a, b) varying concentrations of 4-cyanophenol (4-CN-PhOH, 0–10 μM), and (c,d) varying initial concentrations of target compounds (0.1–5.0 μM) and 5.0 μM 4-cyanophenol. Data for 3,4-dimethoxyphenol (DMOP, from (Remke et al. 2021)) are shown for comparison as open squares in (c) along with TMP data (filled squares). Error bars (when not visible, smaller than the symbol) represent mean deviations of duplicate experiments. Lines indicate (a, b) linear regressions and (c, d) best fits to Eq. (6) with the shaded areas corresponding to 95% confidence intervals.

Moreover, no correction for direct photolysis was necessary for these k^{obs} data due to the minor transformation rates measured in the absence of 2-AN (Table S4a, SI). Consistently for both TCs, $k^{obs}_{0.1}$ was observed to increase linearly with 4-cyanophenol concentration, while $k^{obs}_{5.0}$ was not affected significantly by the presence of 4-cyanophenol. Furthermore, several irradiation experiments were conducted at various initial TC concentrations between 0.1 and 5.0 μM. The corresponding k^{obs}, plotted as a function of the initial TC concentration (Fig. 5c,d), exhibit a hyperbolic decrease, as already observed for DMOP (Remke et al., 2021).

Despite the mentioned similarities, there are several differences in the k^{obs} trends for TMP and aniline. A first difference concerns the slope of the line k^{obs} as a function of [4-CN-PhOH] (Fig. 5a,b), which is about 10 times smaller for aniline than for TMP. This difference in the slope could be due to either a slower electron-transfer reaction between 4-CN-PhO$^{\bullet}$ and aniline compared to TMP, or a less efficient transformation of the formed aniline radical cation to an oxidation product compared to the TMP phenoxyl radical. Aniline radicals or radical cations are known to undergo back-reduction in the presence of antioxidants to form the original compound, which results in a decrease in their transformation rates (Wenk and Canonica 2012, Leresche et al. 2020). In the present experiments, the superoxide radical anion ($O_2^{\bullet-}$), which, according to Scheme 1, is formed during the irradiation of a photosensitizer (such as 2-AN) in the presence of an electron-donor (such as the 4-cyanophenoxide ion, TMP and aniline in the present experiments), could play the antioxidant role by reducing the aniline radical, thereby contributing to a lower transformation rate of aniline. A second important difference is that for aniline (and 4-methylaniline, Fig. S7, SI), $k^{obs}_{5.0} > k^{obs}_{0.1}$ for 4-cyanophenol concentrations below ~2 μM, whereas for TMP $k^{obs}_{5.0} \leq k^{obs}_{0.1}$ for any 4-cyanophenol concentration. In particular, in the absence of 4-cyanophenol, $k^{obs}_{5.0} \cong 7 \times k^{obs}_{0.1}$. This is not explainable based on the kinetic model of Fig. 1, which would predict a pseudo-first-order rate constant independent of initial TC concentration (see discussion below). This anomaly in the photosensitized transformation of aniline might be due to aniline radical (PhNH$^{\bullet}$) coupling reactions of the type described in Eq. (5), which would compete with the back-reduction process, leading to a faster aniline transformation (higher k^{obs}) with increasing [PhNH$^{\bullet}$], and therefore with increasing aniline concentration.

$$PhNH^{\bullet} + PhNH^{\bullet} \rightarrow (PhN)_2 \quad (5)$$

The occurrence of such coupling reactions, leading to the formation of azobenzenes, was found for the transformation of anilines photosensitized by different humic substances (Zepp et al., 1981) and for the oxidation of anilines by manganese dioxide (Laha and Luthy, 1990).

The aforementioned hyperbolic decrease in k^{obs} with increasing initial concentration of TMP and aniline in irradiated solutions containing 2-AN and 4-cyanophenol (5 μM) (Fig. 5c,d) was modeled using a previously developed relationship (Eq. (6)) (Remke et al., 2021).

$$k^{obs}_{TC} = k^{obs}_{^3 2-AN^*,TC} + \beta^{r}_{4-CN-PhO^{\bullet},TC} \Big/ [TC]_0 \quad (6)$$

where k^{obs}_{TC} is the pseudo-first-order rate constant for TC abatement, $k^{obs}_{^3 2-AN^*,TC}$ is the direct contribution of the reaction of TC with the excited triplet state of 2-AN to k^{obs}_{TC}, and $\beta^{r}_{4-CN-PhO^{\bullet},TC}/[TC]_0$ is the contribution of the reaction of TC with the 4-cyanophenoxyl radical to k^{obs}_{TC}, the parameter $\beta^{r}_{4-CN-PhO^{\bullet},TC}$ being an inverse proportionality factor. Non-linear fits of k^{obs}_{TC} vs. $[TC]_0$ according to Eq. (6), are summarized in Table 1.

The second term of the k^{obs}_{TC} calculation in Eq. 6 can also be expressed as:

$$\beta^{r}_{4-CN-PhO^{\bullet},TC} \Big/ [TC]_0 = k^{r}_{4-CN-PhO^{\bullet},TC} \times [4\text{-CN-PhO}^{\bullet}]_{ss} \quad (7)$$

where $k^{r}_{4-CN-PhO^{\bullet},TC}$ is the second-order rate constant for the reaction of TC with 4-CN-PhO$^{\bullet}$ leading to the transformation of TC and [4-CN-PhO$^{\bullet}$]$_{ss}$ is the steady-state concentration of 4-CN-PhO$^{\bullet}$. In turn, [4-CN-PhO$^{\bullet}$]$_{ss}$ can be expressed as the ratio of the rate of its formation, $r^{f}_{4-CN-PhO^{\bullet}}$, and the first-order rate constant for its decay. We assume that, for TMP and DMOP experiments, these compounds are the only scavengers of 4-CN-PhO$^{\bullet}$ present in solution, and that their reaction with TC leads to the transformation of TC with a yield of one. In this case, the following equation holds:

$$[4-CN-PhO^{\bullet}]_{ss} = \frac{r^{f}_{4-CN-PhO^{\bullet}}}{k^{r}_{4-CN-PhO^{\bullet},TC} \times [TC]_0} \quad (8)$$

Substituting Eq. (8) into Eq. (7) and multiplying both sides by $[TC]_0$, yields Eq. (9):

$$\beta^{r}_{4-CN-PhO^{\bullet},TC} = r^{f}_{4-CN-PhO^{\bullet}} \quad (9)$$

These calculations (provided the above assumptions regarding the transformation of TC and the scavenging of 4-CN-PhO$^{\bullet}$ are valid) are able to explain why $\beta^{r}_{4-CN-PhO^{\bullet},TC}$ does not depend on TC ($\beta^{r}_{4-CN-PhO^{\bullet},DMOP} \cong \beta^{r}_{4-CN-PhO^{\bullet},TMP}$) and corresponds to the rate of formation of 4-CN-PhO$^{\bullet}$ for the case of TMP and DMOP.

When comparing the diagrams of TMP and aniline (Fig. 5c,d), it is evident that k^{obs} for aniline cover a much narrower range than for TMP. This is reflected in $\beta^{r}_{4-CN-PhO^{\bullet},Aniline}$, which is more than one order of magnitude lower than $\beta^{r}_{4-CN-PhO^{\bullet},DMOP}$ and $\beta^{r}_{4-CN-PhO^{\bullet},TMP}$. This is a direct consequence of the observations displayed in Fig. 5b and thoroughly discussed above. Despite a good data fit to Eq. (6), aniline cannot be used to estimate $r^{f}_{4-CN-PhO^{\bullet}}$, because its transformation is most probably inhibited by the superoxide radical anion, as discussed in a recent study (Wenk et al., 2021). In addition, aniline transformation is accelerated at higher concentrations, as explained before. Therefore, Eq. (9) is not valid in the case of aniline.

Table 1
Non-linear fits of the observed transformation rate constants of 3,4-dimethoxyphenol (DMOP), 2,4,6-trimethylphenol (TMP) and aniline with varying initial concentrations in irradiated solution containing 2-acetonaphthone (1.5 μM) and 4-cyanophenol (5 μM), buffered at pH 8, according to Eq. 9. Determination coefficients were 0.98, 1.0 and 0.81 for DMOP, TMP and aniline, respectively.

	DMOP	TMP	Aniline
$\beta^{r}_{4-CN-PhO^{\bullet},TC}/M\ s^{-1}$	$(1.23 \pm 0.03) \times 10^{-9}$	$(1.18 \pm 0.01) \times 10^{-9}$	$(1.4 \pm 0.1) \times 10^{-10}$
$k^{obs}_{^3 2-AN^*,TC}/s^{-1}$	$(7.3 \pm 0.1) \times 10^{-4}$	$(2.0 \pm 0.1) \times 10^{-4}$	$(6.5 \pm 0.1) \times 10^{-4}$

3.3. Quenching of the 4-cyanophenoxyl radical by target compounds

Laser flash photolysis experiments were performed primarily to determine second-order rate constants for the quenching of electron-poor phenoxyl radicals by phenols and anilines. The reaction scheme applicable to these experiments is the same as for the photosensitized transformation of a TC in the presence of an electron-poor phenol (Fig. 1b, upper part). Because of the intrinsic difficulty of the experiments, which are impaired by spectral overlap of the various transient species, in particular R-PhO$_{ep}^{\bullet}$ and TC$^{\bullet+}$, experimental series were restricted to the study of the 4-cyanophenoxyl radical. The latter is the main radical investigated in this and a previous study (Remke et al. 2021), and it exhibits a characteristic absorption band with a narrow maximum at 436 nm (Bronner and Wenger 2012; d'Alessandro et al. 2000). The primary selected TC was TMP because of the minor interference caused by absorption of its phenoxyl radical.

Transient absorption spectra obtained by laser flash photolysis of an aerated aqueous solution (pH 8.0) containing 2-AN (150 μM), 4-cyanophenol (2 mM) in the absence or presence of TMP (250 μM) are shown in Fig. 6a or b, respectively. Fig. S9 (SI) represents the simulated regime of transients in this mixture. At a very short delay time (50 ns) after the

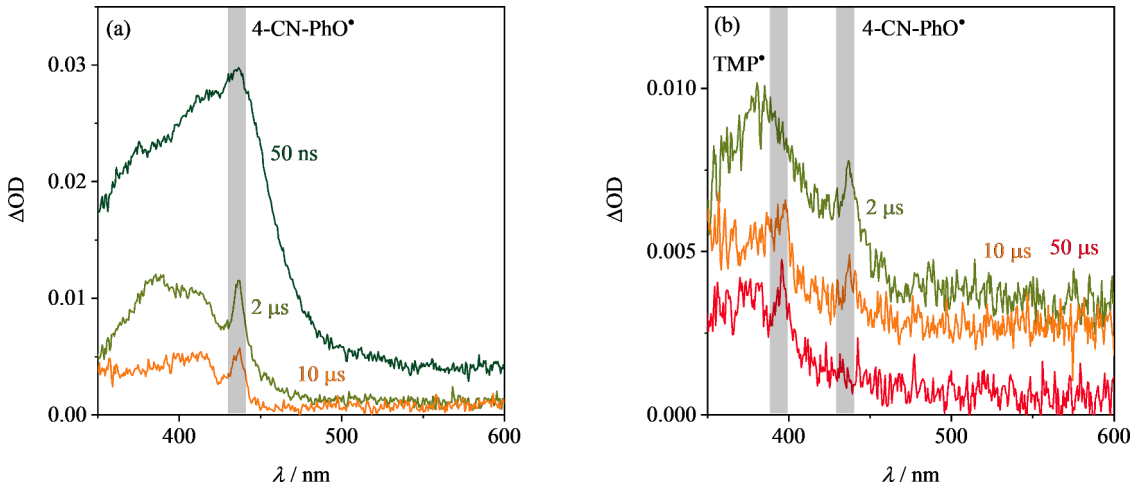

Fig. 6. Transient absorption spectra of an aerated aqueous solution containing (a) 2-acetonaphthone (2-AN, 150 µM) and 4-cyanophenol (4-CN-PhOH, 2 mM). (b) Same as (a) with 2,4,6-trimethylphenol (TMP, 250 µM) as additional solution component.

laser pulse, the transient spectra mainly represent the absorption of ^{3}2-AN* (maximum at ~440 nm) with a small peak at 436 nm corresponding to 4-CN-PhO•. With increasing delay time, the absorption of 4-CN-PhO• becomes clearer and persists in the absence of TMP (Fig. 6a), while the absorption of ^{3}2-AN* strongly decreases and finally disappears. The band at about 390 nm (see 2 µs-delay spectrum) is attributed to the ketyl radical or radical anion of 2-AN, resulting through the electron transfer from 4-CN-PhO$^-$ to ^{3}2-AN*, and disappears at long delay times, mainly due to reaction with oxygen to yield superoxide radical ion (Bryce and Wells 1963). In the presence of TMP (Fig. 6b), the 4-CN-PhO• peak at 436 nm grows until intermediate delay times, then decreases and finally disappears after 50 µs, while a new peak appears at ~395 nm after 10 µs, which persists at least up to 50 µs. This peak is attributed to the phenoxyl radical of TMP, which is formed by the reaction of 4-CN-PhO• with TMP. The just described temporal sequence of species is analogous to the one observed in a previous study about the radical cation of 4-(dimethylamino)benzonitrile and its reaction with phenols and various types of DOM (Leresche et al. 2020). A kinetic model of the main transients formed in the presence of TMP supports this assignment (Text S5 and Fig. S9, SI).

Data obtained using LFP-1. Time delays after the laser pulse are indicated in the diagrams. The excitation wavelength was 355 nm for all of the spectra, samples were buffered at pH 8 with phosphate buffer (20 mM).

The rate of 4-CN-PhO• decay was observed to increase with increasing concentration of the added TMP (see the corresponding absorption traces measured at 436 nm, Figs. S14 and S15, SI). Fitting the decay traces to a single-exponential function with a constant offset yielded first-order rate constants that increased with increasing TMP concentration (Fig. 7b).

First, we consider the value of the first-order decay rate constant of 4-CN-PhO• in the absence of TMP (i.e., for [TMP] = 0), which is close to 2.5×10^4 s^{-1}. This value corresponds to a lifetime of ~40 µs for 4-CN-PhO• under the present laser flash photolysis experimental conditions. The lifetime of 4-CN-PhO• under the conditions used for steady-state irradiation is probably significantly higher than this, since the concentration of reactive radical species that could contribute to its quenching (such as 4-CN-PhO• itself, Sens$^{\bullet-}$ and $O_2^{\bullet-}$) is much lower. Consequently, 4-CN-PhO• is a "long-lived" species compared to the excited triplet state of any photosensitizer in aerated aqueous solution and is appropriate, from this point of view, as an LLPO surrogate. Second, linear regression lines of the aforementioned first-order rate constants

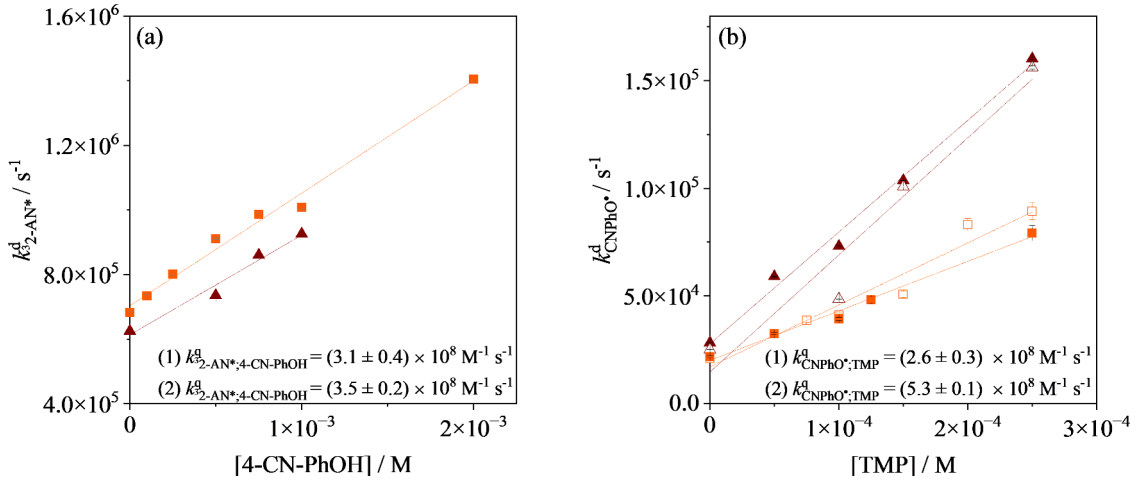

Fig. 7. First-order decay rate constants, determined in aerated aqueous solution of 2-acetonphahtone ([2-AN]$_0$ = 150 µM), of (a) ^{3}2-AN* as a function of the 4-cyanophenol (4-CN-PhOH) concentration, used to determine the corresponding second-order quenching rate constants, $k^q_{^3\text{2-AN*,4-CN-PhOH}}$, by linear regression (lines), and (b) 4-CN-PhO• ([4-CN-PhOH]$_0$ = 1 mM) as a function of the 2,4,6-trimethylphenol (TMP) concentration, used to determine the corresponding second-order quenching rate constants, $k^q_{\text{4-CN-PhO•,TMP}}$ by linear regression (lines).

(Fig. 7b) were used to determine the second-order rate constant for the quenching of 4-CN-PhO$^\bullet$ by TMP, $k^q_{4-CN-PhO^\bullet,TMP}$. Values of $k^q_{4-CN-PhO^\bullet,TMP}$ of (2.6 ± 0.3) × 10^8 M^{-1} s^{-1} and (5.3 ± 0.1) × 10^8 M^{-1} s^{-1} for measurements performed using the instruments LFP-1 and LFP-2, respectively, were obtained. An experimental series performed using deuterated water as a solvent and LFP-1 yielded $k^q_{4-CN-PhO^\bullet,TMP}$ = (1.68 ± 0.09) × 10^8 M^{-1} s^{-1}, from which a deuterium isotope effect of 1.5 ± 0.3 was derived. This suggests that a proton, either from the solvent or from the phenolic functional group of TMP, is involved in the rate determining step of the reaction between 4-CN-PhO$^\bullet$ and TMP.

Open and filled symbols represent two distinct measurement series performed using the same equipment. Orange squares and rate constants: data obtained using LFP-1; dark brown triangles and rate constants: data obtained using LFP-2. Excitation wavelength was 355 nm for all of the measurements, samples were buffered at pH 8 with phosphate buffer (20 mM).

The reason why two significantly different $k^q_{4-CN-PhO^\bullet,TMP}$ values using different instruments were obtained could be due to the different signal intensities, which were higher for LFP-2 than for LFP-1. Taking the higher value of (5.3 ± 0.1) × 10^8 M^{-1} s^{-1} as a limit for a higher estimate, one can definitely state that it is much lower than typical diffusion-controlled rate constants for the reaction of phenoxyl radicals with electron donors, i.e. ~4 × 10^9 M^{-1} s^{-1} (Neta and Grodkowski, 2005). This conclusion matches with the prediction made in Section 3.1 about the magnitude of $k^q_{4-CN-PhO^\bullet,TMP}$. Unfortunately, for DMOP the determination of the corresponding rate constant was not possible because of the superposition of the UV-Vis absorption bands of the DMOP phenoxl radical and 4-CN-PhO$^\bullet$. In view of the conclusions of Section 3.1 and the lower value of $E^0_{red,1}$ for DMOP compared to TMP, it is very likely that $k^q_{4-CN-PhO^\bullet,DMOP} > k^q_{4-CN-PhO^\bullet,TMP}$. Analogous laser flash photolysis experiments were performed using aniline and 4-methylaniline as target compounds. In solution containing 2-AN as a photosensitizer and 4-CN-PhOH as an electron-poor phenol, the formation of the corresponding aniline radicals or radical cations could be observed (Fig. S8 c–f, SI). However, the determination of second-order rate constant for the reaction of 4-CN-PhO$^\bullet$ with these anilines was not successful due to strong spectral overlap caused by these radicals.

Additional experiments were performed to determine second-order rate constants for the quenching of ^{3}2-AN* by the 4-cyanophenol (Fig. 7a), aniline and 4-methylaniline (4-MA) (Table 2). The transient absorption decay traces of ^{3}2-AN*, measured at 440−450 nm, were fitted to single-exponential functions to obtain the corresponding first-order quenching rate constants (Figs. S11−13, SI). The latter were then plotted against quencher concentration to determine second-order rate constants as the slope of the corresponding linear regression lines. The rate constants for the quenching of triplet state 2-acetonaphtone are summarized in Table 2 (Fig. S10, SI). The values determined for 4-cyanophenol with the two different laser flash photolysis instruments are identical within experimental error and lead to an average value of $k^q_{^32-AN^*,4-CN-PhOH}$ = (3.3 ± 0.3) × 10^8 M^{-1} s^{-1}, measured at pH 8.0 (Fig. 7a). Assuming that quenching is due exclusively to the 4-cyanophenoxide ion and considering the speciation of 4-cyanophenol, the quenching rate constant for the 4-cyanophenoxide ion can be estimated as $k^q_{^32-AN^*,4-CN-PhO^-}$ = (6.6 ± 0.6) × 10^8 M^{-1} s^{-1}. This value is about half of the value that can be extrapolated from a previous, less precise rate constant determined at pH 6.0 (Canonica et al. 2000). For the anilines, second-order quenching rate constants are not far from the diffusion controlled limit, but about 30% lower compared to corresponding values previously measured for DMOP and trolox (Canonica et al. 2000), and within the range of values determined for the quenching of the excited triplet state of methylene blue by various anilines at pH 8.4 (Erickson et al. 2015).

Table 2
Quenching rate constants for the 4-cyanophenoxyl radical and triplet state 2-acetonaphthone.

Quencher (Q)	$k^q_{4-CN-PhO^\bullet,Q}$ / $M^{-1}s^{-1}$	
TMP	(4 ± 1) × 10^8	(this study)
Ascorbate ion	2 × 10^9	Schuler (1977)
	$k^q_{^32-AN^*,Q}$/$M^{-1}s^{-1}$	
4-CN-PhOH	(3.3 ± 0.3) × 10^8 (pH 8)	(this study)
	(1.3 ± 1.3) × 10^7 (pH 6)	Canonica et al. (2000)
Aniline	(1.9 ± 0.3) × 10^9	(this study)
4-methylaniline	(1.9 ± 0.1) × 10^9	(this study)
3,4-dimethoxyphenol	(3.1 ± 0.1) × 10^9	Canonica et al. (2000)
trolox	(2.7 ± 0.2) × 10^9	Canonica et al. (2000)

4. Environmental implications

The motivation of this study was to characterize the still elusive DOM-derived long-lived photooxidants (LLPO), and to test the hypothesis that they may consist of electron-poor phenoxyl radicals. The applied model systems to mimic LLPO were solutions containing a model photosensitizer and an electron-poor phenol. Irradiation experiments were performed under the same conditions as many previous experiments using CDOM as a source of photooxidants. Thereby, electron-poor phenoxyl radicals were produced, which were observed to induce the transformation of typical target compounds subject to LLPO effect.

All investigated electron-poor phenoxyl radicals, having reduction potentials in the range of 0.85−1.12 V vs. SHE, lead to a significant enhancement in the photosensitized transformation of the LLPO probe compounds DMOP and TMP. This fact suggests that the lower limit of $E^0_{red,1}$ of DOM-derived LLPO might be lower than the previously estimated value of 1.0 V (Remke et al., 2021). Moreover, the determined second-order rate constant for the reaction of TMP with 4-CN-PhO$^\bullet$ ((4 ± 1) × 10^8 M^{-1} s^{-1}) was well below the diffusion-controlled limit. For the other studied phenoxyl radicals, having lower $E^0_{red,1}$ values compared to the 4-CN-PhO$^\bullet$, lower rate constants for their reaction with TMP are expected. Therefore, having second-order rate constants near the diffusion-controlled limit does not appear to be required for an enhancement of the phototransformation of LLPO probe compounds under steady-state irradiation due to the presence of phenoxyl radicals. In conclusion, the estimation of $E^0_{red,1}$ of LLPO based on the oxidation potentials of probe compounds (Remke et al., 2021) and on $E^0_{red,1}$ values of model oxidants (in the present study, electron-poor phenoxyl radicals) is not straightforward and needs further investigation.

The formation pathways of LLPO during irradiation of CDOM are still unknown. One possible pathway, which was modelled in the present study, assumes LLPO to be formed by reaction of ^{3}Sens* (as a surrogate for ^{3}CDOM*) with electron-poor phenols. Using ^{3}CBBP* and ^{3}2-AN* as ^{3}CDOM* surrogates with high and low $E^0_{red,1}$, respectively, two different behaviors in the effect of electron-poor phenoxyl radicals on phenolic TCs transformation were observed: (1) with ^{3}CBBP*, an increase in phototransformation that was related to an increase in $E^0_{red,1}$ of the electron-poor phenoxyl radicals, with an assumed uniform production rate of all these radicals, and (2) with ^{3}2-AN*, an increase in phototransformation that was mainly related to an increase of the degree of deprotonation of the electron-poor phenols. Since $E^0_{red,1}$ of ^{3}CDOM* spans a wide range covering the values for ^{3}CBBP* and ^{3}2-AN*, both of the above behaviors are expected to occur concomitantly in irradiated CDOM solution. The contribution of a ^{3}2-AN*-like behavior agrees with the observed increase of the LLPO effect with increasing pH (Canonica and Freiburghaus, 2001). Such a pH effect would also be compatible with direct photoionization of phenoxides as electron-poor phenoxyl radical source (see Eq. 4), since phenoxides have increased light

absorption (Fig. S3, SI) and photoionization quantum yields compared to the corresponding undissociated phenols (Grabner et al., 1977). Both effects lead to increased rates of phenoxyl radical production from phenoxides compared to phenols.

Transformation rates of aniline and 4-methylaniline due to reaction with 4-CN-PhO$^{\bullet}$ were observed to be much lower than the corresponding rates for TMP and DMOP. This would suggest a reduced importance of LLPO in the phototransformation of anilines compared to electron-rich phenols. Also, for model systems with ^{3}2-AN* and 4-CN-PhO$^{\bullet}$ as model photooxidants, the enhancement of aniline transformation by reducing the initial concentration of aniline from 5.0 to 0.1 μM was much smaller than for the phenolic TCs. This effect, attributed to a complex behavior in the photosensitized transformation of the anilines (which appears to be influenced by autocatalysis in the studied initial concentration range), is able to explain the low enhancement factors observed using Suwannee River fulvic acid as source of ^{3}CDOM* and LLPO (Remke et al., 2021). Moreover, these observations suggest that indirect phototransformation kinetics of anilines should be measured at very low concentrations ($\leq$ 0.1 μM) to make accurate predictions on the fate of anilines in sunlit surface waters.

5. Conclusions

In this study target compound transformation mediated by various photochemically produced electron-poor phenoxyl radicals was investigated. The transformation of the electron-rich compounds, 3,4-dimethoxyphenol and 2,4,6-trimethylphenol, aniline and 4-methylaniline was monitored in aqueous solutions of DOM model systems, each consisting of an aromatic ketone as photosensitizer and an electron-poor phenol as LLPO precursor.

- For a low initial concentration (0.1 μM) of the target compounds, higher transformation rate constants were observed compared to a higher initial concentration (5.0 μM), confirming the involvement of long-lived reactive species assumed to be photochemically produced electron-poor phenoxyl radicals.
- With increasing $E^{0}_{\mathrm{red},1}$ of the employed phenoxyl radicals, faster transformations of phenolic target compounds were observed, while the selectivity of the phenoxyl radicals decreased.
- The formation rate of phenoxyl radicals from electron-poor phenols was shown to be controlled by both the one-electron reduction potential of the excited triplet state of the photosensitizer and the fraction of the electron-poor phenoxide.
- The rates of aniline and 4-methylaniline transformation induced by photochemically produced 4-cyanophenoxyl radical were significantly lower than for the transformation of phenolic target compounds. This is interpreted as an indication that transformation of anilines is probably hampered by back-reduction of their radical oxidation intermediates through reductants, primarily the superoxide radical ion.
- The second-order rate constant for the quenching of 4-cyanophenoxyl radical by 2,4,6-trimethylphenol in aqueous solution was determined as $(4 \pm 1) \times 10^{8}$ $M^{-1}s^{-1}$. The moderate but significant deuterium isotope effect for this rate constant (~1.5) indicates a proton coupled electron transfer in the rate-determining step of the reaction.
- The results of this study are crucial to understand the nature of LLPO generated by irradiation of CDOM solutions. For instance, they enabled an estimation of reduction potentials of LLPO, and provided possible explanations for the previously observed pH dependence of the LLPO effect and low enhancement factors for anilines in irradiated CDOM solutions.

Funding

This study was supported by the Swiss National Science Foundation (Project No. 200021-169422) and by the Czech Science Foundation via project GA 19-08239S.

Supplementary materials Supplementary material associated with this article can be found, in the online version, at doi:

Declaration of Competing Interest

The authors declare that they have no known competing financial interests or personal relationships that could have appeared to influence the work reported in this paper.

Silvio Canonica reports financial support was provided by Swiss National Science Foundation. Dominik Heger reports financial support was provided by Czech Science Foundation.

Acknowledgements

The authors would like to thank Ursula Schönenberger and Elisabeth Salhi for technical and laboratory support.

Supplementary materials

Supplementary material associated with this article can be found, in the online version, at doi:10.1016/j.watres.2022.118095.

References

Bronner, C., Wenger, O.S., 2012. Proton-coupled electron transfer between 4-cyanophenol and photoexcited rhenium (I) complexes with different protonatable sites. Inorg. Chem. 51 (15), 8275–8283.
Bryce, W., Wells, C., 1963. The flash photolytic reduction of 2-acetonaphthone in solution. Can. J. Chem. 41 (10), 2722–2727.
Buschmann, J., Canonica, S., Lindauer, U., Hug, S.J., Sigg, L., 2005a. Photoirradiation of dissolved humic acid induces arsenic (III) oxidation. Environ. Sci. Technol. 39 (24), 9541–9546.
Buschmann, J., Canonica, S., Sigg, L., 2005b. Photoinduced oxidation of antimony (III) in the presence of humic acid. Environ. Sci. Technol. 39 (14), 5335–5341.
Canonica, S., Freiburghaus, M., 2001. Electron-rich phenols for probing the photochemical reactivity of freshwaters. Environ. Sci. Technol. 35 (4), 690–695.
Canonica, S., Hellrung, B., Wirz, J., 2000. Oxidation of phenols by triplet aromatic ketones in aqueous solution. J. Phys. Chem. A 104 (6), 1226–1232.
Canonica, S., Hoigné, J., 1995. Enhanced oxidation of methoxy phenols at micromolar concentration photosensitized by dissolved natural organic material. Chemosphere 30 (12), 2365–2374.
Canonica, S., Jans, U., Stemmler, K., Hoigné, J., 1995. Transformation kinetics of phenols in water: photosensitization by dissolved natural organic material and aromatic ketones. Environ. Sci. Technol. 29 (7), 1822–1831.
Canonica, S., Tratnyek, P.G., 2003. Quantitative structure-activity relationships for oxidation reactions of organic chemicals in water. Environ. Toxicol. Chem. 22 (8), 1743–1754.
Carena, L., Puscasu, C.G., Comis, S., Sarakha, M., Vione, D, 2019. Environmental photodegradation of emerging contaminants: a re-examination of the importance of triplet-sensitised processes, based on the use of 4-carboxybenzophenone as proxy for the chromophoric dissolved organic matter. Chemosphere 237, 124476.
d'Alessandro, N., Giorgio, B., Fang, X., Jin, F., Schuchmann, H.P., von Sonntag, C, 2000. Reaction of superoxide with phenoxyl-type radicals. J. Chem. Soc. 2, 1862–1867. Perkin Transactions.
Das, P.K., Bhattacharyya, S.N., 1981. Laser flash photolysis study of electron transfer reactions of phenolate ions with aromatic carbonyl triplets. J. Phys. Chem. 85 (10), 1391–1395.
Erickson, P.R., Walpen, N., Guerard, J.J., Eustis, S.N., Arey, J.S., McNeill, K., 2015. Controlling factors in the rates of oxidation of anilines and phenols by triplet methylene blue in aqueous solution. J. Phys. Chem. A 119 (13), 3233–3243.
Grabner, G., Köhler, G., Zechner, J., Getoff, N., 1977. Pathways for formation of hydrated electrons from excited phenol and related compounds. Photochem. Photobiol. 26 (5), 449–458.
Ianni, J.C. (2017) Kintecus. Windows Version 6.01 www.kintecus.com.
Laha, S., Luthy, R.G., 1990. Oxidation of aniline and other primary aromatic amines by manganese dioxide. Environ. Sci. Technol. 24 (3), 363–373.
Laszakovits, J.R., Berg, S.M., Anderson, B.G., O'Brien, J.E., Wammer, K.H., Sharpless, C. M., 2017. p-Nitroanisole/pyridine and p-nitroacetophenone/pyridine actinometers revisited: quantum yield in comparison to ferrioxalate. Environ. Sci. Technol. Lett. 4 (1), 11–14.
Leenheer, J.A., Croué, J.P., 2003. Characterizing aquatic dissolved organic matter. Environ. Sci. Technol. 37 (1), 18A–26A.

Leresche, F., Ludvíková, L., Heger, D., Klán, P., von Gunten, U., Canonica, S., 2019. Laser flash photolysis study of the photoinduced oxidation of 4-(dimethylamino) benzonitrile (DMABN). Photochem. Photobiol. Sci. 18 (2), 534–545.
Leresche, F., Ludvíková, L.., Heger, D., von Gunten, U., Canonica, S., 2020. Quenching of an aniline radical cation by dissolved organic matter and phenols: A laser flash photolysis study. Environ. Sci. Technol. 54 (23), 15057–15065.
Leresche, F., von Gunten, U., Canonica, S., 2016. Probing the photosensitizing and inhibitory effects of dissolved organic matter by using N, N-dimethyl-4-cyanoaniline (DMABN). Environ. Sci. Technol. 50 (20), 10997–11007.
Li, C., Hoffman, M.Z., 1999. One-electron redox potentials of phenols in aqueous solution. J. Phys. Chem. B 103 (32), 6653–6656.
Lind, J., Shen, X., Eriksen, T.E., Merenyi, G., 1990. The one-electron reduction potential of 4-substituted phenoxyl radicals in water. J. Am. Chem. Soc. 112 (2), 479–482.
McNeill, K., Canonica, S., 2016. Triplet state dissolved organic matter in aquatic photochemistry: reaction mechanisms, substrate scope, and photophysical properties. Environ. Sci.: Processes Impacts 18 (11), 1381–1399.
Neta, P., Grodkowski, J., 2005. Rate constants for reactions of phenoxyl radicals in solution. J. Phys. Chem. Ref. Data 34 (1), 109–199.
Ossola, R., Jonsson, O.M., Moor, K., McNeill, K., 2021. Singlet oxygen quantum yields in environmental waters. Chem. Rev. 121 (7), 4100–4146.
Remke, S.C., von Gunten, U., Canonica, S., 2021. Enhanced transformation of aquatic organic compounds by long-lived photooxidants (LLPO) produced from dissolved organic matter. Water Res. 190, 116707. Article.
Richard, C., Canonica, S., Hutzinger, O., 2005. The Handbook of Environmental Chemistry, ed. Springer, Berlin, Germany, pp. 299–323.
Schuler, R.H., 1977. Oxidation of ascorbate anion by electron transfer to phenoxyl radicals. Radiat. Res. 69 (3), 417–433.
Steenken, S., Neta, P., 2003. The Chemistry of Phenols. Wiley, New York.
Vione, D., Minella, M., Maurino, V., Minero, C., 2014. Indirect photochemistry in sunlit surface waters: photoinduced production of reactive transient species. Chem. Eur. J. 20 (34), 10590–10606.
Wenk, J., Canonica, S., 2012. Phenolic antioxidants inhibit the triplet-induced transformation of anilines and sulfonamide antibiotics in aqueous solution. Environ. Sci. Technol. 46 (10), 5455–5462.
Wenk, J., Graf, C., Aeschbacher, M., Sander, M., Canonica, S., 2021. Effect of solution pH on the dual role of dissolved organic matter in sensitized pollutant photooxidation. Environ. Sci. Technol. 55 (22), 15110–15122.
Zark, M., Dittmar, T., 2018. Universal molecular structures in natural dissolved organic matter. Nat. Commun. 9 (1), 1–8.
Zepp, R.G., Baughman, G.L., Schlotzhauer, P.F., 1981. Comparison of photochemical behavior of various humic substances in water: I. Sunlight induced reactions of aquatic pollutants photosensitized by humic substances. Chemosphere 10 (1), 109–117.